# The structure of the Ekman layer for geostrophic flows with lateral shear[1]

By GEORGE S. BENTON, FRANK B. LIPPS,[2] and SHIH-YU TUANN, *The Johns Hopkins University, Baltimore, Md.*

(Manuscript received November 25, 1963)

ABSTRACT

A generalized Ekman flow is obtained for the boundary layer of a semi-infinite, rotating homogeneous fluid with lateral variation in the horizontal velocity components far from the boundary surface. The fields of motion considered include uni-directional motion with lateral shear, symmetric and elongated eddies, and cols. A solution for the first of these cases is obtained to fifth order; for the others, to second order. In all cases the magnitude of the vertical velocities induced by convergence in the boundary layer is greater for systems with negative relative vorticity than for systems with positive relative vorticity. The result differs substantially from first-order theory, for which the magnitude of the vertical velocity is proportional to the relative vorticity. A number of meteorological applications are considered.

## 1. Introduction

The importance of boundary layer flows in the mechanics of rotating fluids is well known. In a homogeneous fluid in strong rotation, motion is essentially geostrophic outside of the boundary layer and the velocity components do not change in a direction parallel to the axis of rotation. Thus, a substantial part of the cross-isobaric transport of fluid occurs in a thin layer near the boundaries of the system.

The structure of the boundary layer in a homogeneous rotating fluid was first examined by EKMAN (1905) who derived the velocity field resulting from a semi-infinite, uniform current in geostrophic equilibrium moving over a plane surface. The Ekman solution has played an important part in our effort to understand behavior of geophysical fluid systems, both in the field and in the laboratory. In these efforts, the effect of lateral variations in geostrophic flow has often been dealt with qualitatively. The cross-isobaric mass transport in the Ekman layer is proportional to the geostrophic speed, and it has long been recognized that when the latter quantity varies in space, an inevitable result will be the establishment of lateral divergence or convergence in the boundary layer. This, in turn, leads to vertical velocities which may be of substantial geophysical importance.

Despite the importance of the boundary layer in the mechanics of geophysical fluids, surprisingly little has been done on the effects of frictional drag in a system with lateral variation in the geostrophic flow. A first order approximation, neglecting inertia terms, indicates that the vertical velocity at the top of the boundary layer is proportional to the relative vorticity (CHARNEY and ELIASSEN, 1949). More detailed analyses have been developed for systems with radial symmetry. Thus, for example, BOEDEWADT (1940) studied the boundary layer in a fluid in solid rotation above a plate, and ROGERS and LANCE (1960) extended the problem to a plate rotating at an angular velocity different from the fluid. The stability of boundary layers in a symmetric vortex has been examined experimentally by FALLER (1962). Nevertheless, much remains to be accomplished in evaluating the effect of frictional drag in these and other types of flow fields.

In the present study, the equations of motion are examined for a semi-infinite rotating fluid in which the horizontal velocity components are linear functions of the Cartesian coordinates parallel to a plane (horizontal) boundary. With

[1] This research was supported by a grant (NSF G-14707) from the National Science Foundation.

[2] Now at the University of Chicago, Chicago, Illinois.

these assumptions it is shown that the Navier-Stokes' equations reduce to a set of partial differential equations in which the only space coordinate is the one perpendicular to the boundary. If steady-state flow is assumed, the equations reduce further to a set of ordinary non-linear differential equations. This was first shown by LIN (1958) in connection with the motion of an electrically conducting fluid in a magnetic field. Lin's development is equally applicable to geophysical problems where the Coriolis forces appear due to the earth's rotation.

The class of problems examined below includes the radially symmetric vortex as a special case. Also included are: elliptic vortices, "cols" (the region near the stagnation point between two pairs of eddies with opposing angular velocity), and uni-directional flow with horizontal velocity shear. All of these types of flow are of substantial geophysical interest.

## 2. Formulation of Equations of Motion

It will be assumed that we are dealing with a semi-infinite, rotating fluid moving over a plane surface ($z = 0$). We will also assume that the horizontal velocity components are each linear in the horizontal space variables; and that the pressure is quadratic in these variables. From the equation of continuity we can conclude that the vertical velocity component is a function of $z$ only. Thus it is consistent with the continuity equation to write:

$$\begin{aligned} u &= E'(z,t) + A'(z,t)\,y + B_z'(z,t)\,x, \\ v &= F'(z,t) + C_z'(z,t)\,y + D'(z,t)\,x, \\ w &= -B'(z,t) - C'(z,t), \\ \frac{p}{\varrho} &= a'x + b'y + \frac{k'}{2}x^2 + l'xy - \frac{m'}{2}y^2 + G'(z,t), \end{aligned} \tag{1}$$

where $(u, v, w)$ are the $(x, y, z)$ velocity components; $p$ is the pressure and $\varrho$ is the density. With appropriate choice of the origin and with suitable orientation of the horizontal axes, the above equations can be written in the following form without loss in generality:

$$\begin{aligned} u &= E(z,t) + A(z,t)\,y + B_z(z,t)\,x, \\ v &= F(z,t) + C_z(z,t)\,y + D(z,t)\,x, \\ w &= -B(z,t) - C(z,t), \\ \frac{p}{\varrho} &= \frac{k}{2}x^2 - \frac{m}{2}y^2 + G(z,t). \end{aligned} \tag{2}$$

These relationships can be substituted into the Navier-Stokes' Equation to obtain a set of seven partial differential equations in $(z, t)$ However, further simplification is desirable.

Let us consider steady flows which become non-divergent and independent of the vertical coordinate as $z$ becomes indefinitely large. From the symmetry of the pressure field it is reasonable to seek solutions for which the horizontal velocity components are odd functions of $(x, y)$ so that $E = F = 0$. With these simplifications, substitution of Equations (2) into the Navier-Stokes' equation for a rotating fluid with a vertical axis of rotation yields the following five ordinary differential equations in five unknown functions:

$$\begin{aligned} \dot{B}^2 - B\ddot{B} + AD - \ddot{B}C &= -k + fD + \nu\dddot{B}, \\ A\dot{B} - \dot{A}B + A\dot{C} - \dot{A}C &= f\dot{C} + \nu\ddot{A}, \\ \dot{B}D - B\dot{D} + \dot{C}D - C\dot{D} &= -f\dot{B} + \nu\ddot{D}, \\ \dot{C}^2 - C\ddot{C} + AD - B\ddot{C} &= m - fA + \nu\dddot{C}, \\ \dot{G} &= -(B+C)(\dot{B}+\dot{C}) + \nu(\ddot{B}+\ddot{C}) - g, \end{aligned} \tag{3}$$

where $\nu$ is the kinematic viscosity; $f$ is the Coriolis parameter; $g$ is the acceleration due to gravity; and the dots denote total differentiation with respect to $z$. These equations are to be solved under the boundary conditions that the fluid velocity is zero at $z = 0$ and that the flow becomes non-divergent $(B_z + C_z = 0)$ and independent of the vertical coordinate $(A_z = B_{zz} = C_{zz} = D_z = 0)$ at $z = \infty$.

It will be convenient to non-dimensionalize these equations in terms of the two parameters $f$ and $\nu$. Thus, introducing the non-dimensional variables:

$$\begin{aligned} (u^*, v^*, w^*) &= (u(f\nu)^{-\frac{1}{4}}, v(f\nu)^{-\frac{1}{4}}, w(f\nu)^{-\frac{1}{4}}), \\ z^* &= \frac{1}{\sqrt{2}}\,z\left(\frac{f}{\nu}\right)^{\frac{1}{4}}, \\ k^* &= \frac{k}{f^2}, \qquad m^* = \frac{m}{f^2}. \\ B^* &= \frac{1}{\sqrt{2}}\,B(f\nu)^{-\frac{1}{4}}, \quad C^* = \frac{1}{\sqrt{2}}\,C(f\nu)^{-\frac{1}{4}}, \\ A^* &= \frac{A}{f}, \qquad D^* = \frac{D}{f}. \end{aligned} \tag{4}$$

one obtains finally after dropping the asterisks:

$$\begin{aligned} &\dot{B}^2 - B\ddot{B} + AD - \ddot{B}C = -k + D + \tfrac{1}{2}\dddot{B}, \\ &A\dot{B} - \dot{A}B + A\dot{C} - \dot{A}C = \dot{C} + \tfrac{1}{2}\ddot{A}, \\ &\dot{B}D - B\dot{D} + \dot{C}D - C\dot{D} = -\dot{B} + \tfrac{1}{2}\ddot{D}, \\ &\dot{C}^2 - C\ddot{C} + AD - B\ddot{C} = m - A + \tfrac{1}{2}\dot{C}, \end{aligned} \tag{5}$$

where the third equation of motion, describing pressure variations in the vertical, has been dropped, and where:

$$\begin{aligned} &A = B = C = D = \dot{B} = \dot{C} = 0 \quad \text{at} \quad z = 0, \\ &\dot{B} + \dot{C} = 0 \quad \text{and} \\ &\dot{A} = \ddot{B} = \ddot{C} = \dot{D} = 0 \qquad \text{at} \quad z = \infty. \end{aligned}$$

These equations represent a variety of asymptotic flows, depending on the choice of the parameters $(k, m)$ describing the horizontal pressure variation.

## 3. Asymptotic flows wich are uniform, with constant horizontal shear

Let us first consider shear flow of a semi-infinite rotating fluid moving over a horizontal plane. For this special case $m = 0$, if the horizontal pressure gradient is assumed to be parallel to the $x$-axis. From symmetry, we may assume $A = C \equiv 0$. Equations (5) become:

$$\begin{aligned} &\dot{B}^2 - B\ddot{B} = -k + D + \tfrac{1}{2}\dddot{B}, \\ &\dot{B}D - B\dot{D} = -\dot{B} + \tfrac{1}{2}\ddot{D}. \end{aligned} \tag{6}$$

where $B = \dot{B} = D = 0$; at $z = 0$,

$\dot{B} = \dot{D} = 0$; at $z = \infty$.

These are simultaneous, ordinary, non-linear differential equations with a single non-dimensional parameter $k$, the ratio of horizontal velocity shear to the vorticity associated with the rotating coordinate system. Thus, $(k + 1)$ is the absolute vorticity at $z = \infty$, in appropriate nondimensional form.

Let us assume the following expansion for the unknown functions $B(z)$ and $D(z)$:

$$\begin{aligned} B(z) &= \sum_{n=1}^{\infty} k^n B_n(z), \\ D(z) &= \sum_{n=1}^{\infty} k^n D_n(z). \end{aligned} \tag{7}$$

Inserting these expressions into (6) and equating the coefficients of like powers of the parameter $k$, we obtain a set of ordinary differential equations for the functions $B_n(z)$ and $D_n(z)$, the first three of which are:

$$k: \quad \begin{aligned} &\tfrac{1}{2}\dddot{B}_1 + D_1 = 1, \\ &\tfrac{1}{2}\ddot{D}_1 - \dot{B}_1 = 0. \end{aligned} \tag{a}$$

$$k^2: \quad \begin{aligned} &\tfrac{1}{2}\dddot{B}_2 + D_2 = \dot{B}_1^2 - B_1\ddot{B}_1, \\ &\tfrac{1}{2}\ddot{D}_2 - \dot{B}_2 = \dot{B}_1 D_1 - B_1\dot{D}_1. \end{aligned} \tag{b}$$

$$k^3: \quad \begin{aligned} &\tfrac{1}{2}\dddot{B}_3 + D_3 = 2\dot{B}_1\dot{B}_2 - (B_1\ddot{B}_2 + \ddot{B}_1 B_2), \\ &\tfrac{1}{2}\ddot{D}_3 - \dot{B}_3 = (\dot{B}_1 D_2 + \dot{B}_2 D_1) - (B_1\dot{D}_2 + B_2\dot{D}_1). \end{aligned} \tag{c}$$

(8)

Or, in general:

$$\begin{aligned} \tfrac{1}{2}\dddot{B}_n + D_n &= \sum_{m=1}^{n-1} (\dot{B}_m\ddot{B}_{n-m} - B_m\dddot{B}_{n-m}), \\ \tfrac{1}{2}\ddot{D}_n - \dot{B}_n &= \sum_{m=1}^{n-1} (\dot{B}_m D_{n-m} - B_m\dot{D}_{n-m}). \end{aligned} \tag{9}$$

The boundary conditions for $B_n$ and $D_n$ are:

$$\begin{aligned} &\text{At } z = 0: \; B_n = \dot{B}_n = D_n = 0 \quad \text{for all} \quad n; \\ &\text{At } z = \infty: \; \dot{B}_1 = 0, \; D_1 = 1, \\ &\qquad\qquad \dot{B}_n = 0, \; D_n = 0, \quad \text{for} \quad n \geqslant 2. \end{aligned} \tag{10}$$

Let us now obtain solutions in closed form for the first few functions $B_n(z)$ and $D_n(z)$. As is evident from (8$a$), the equations for $B_1(z)$ and $D_1(z)$ are identical in form with those of the Ekman problem, except that the function $\dot{B}_1$ replaces the $u$-component of the velocity in the Ekman flow, and the function $D_1$ replaces the $v$-component. The solution, subject to the appropriate boundary conditions, is:

$$\begin{aligned} B_1 &= -\tfrac{1}{2} + \tfrac{1}{2}e^{-z}(\cos z + \sin z), \\ \dot{B}_1 &= -e^{-z}\sin z, \\ D_1 &= 1 - e^{-z}\cos z. \end{aligned} \tag{11}$$

A physical interpretation of these results is straightforward. At each value of $x$, the first-order solution is such that the horizontal velocity components follow exactly the Ekman flow pattern. However, the magnitude of these horizontal velocity components varies linearly in the $x$-direction. As a result of friction, a vertical velocity component is set up which is independent of the x-coordinate. As $z$ approaches infinity, this yields an asymptotic vertical velocity $w = k/2$, where $k = (\partial v/\partial x)/f$. This result is presented graphically in Fig. 3. It is to be noted that the friction-induced vertical velocities are positive in the vicinity of a trough (low pressure, $k$ positive), and are negative in the vicinity of a ridge (high pressure, $k$ negative). The first-order solution yields vertical velocities of the same magnitude for anticyclonic and cyclonic shears of equivalent strength. Furthermore, the vertical velocity is directly proportional to the relative vorticity.

The second-order solution is obtained from substituting (11) into (8$b$). After straightforward but lengthy integration, one obtains:

$$B_2 = \frac{7}{40} - \frac{3}{20}e^{-2z} - \frac{1}{40}e^{-z}(\cos z + 23 \sin z) + \frac{z}{4}e^{-z}\cos z,$$

$$\dot{B}_2 = \frac{3}{10}e^{-2z} - \frac{1}{10}e^{-z}(3\cos z - 6\sin z) - \frac{1}{4}ze^{-z}(\cos z + \sin z), \tag{12}$$

$$D_2 = -\frac{1}{10}e^{-2z} + \frac{1}{10}e^{-z}(\cos z + 3\sin z) - \frac{1}{4}ze^{-z}(\cos z - \sin z).$$

Thus, the asymptotic vertical velocity can be written in non-dimensional form as:

$$w = \frac{1}{2}k - \frac{7}{40}k^2. \tag{13}$$

A difference in behavior is evident between cases of anticyclonic and cyclonic shear: the magnitude of the vertical velocity is greater for anticyclonic ($k < 0$) than for cyclonic ($k > 0$) shear for systems of equivalent strength.

The third-order solution is even more lengthy. It is

$$B_3 = -\frac{15}{320} - \frac{3}{40}ze^{-2z} + \frac{39}{400}e^{-2z} + \frac{1}{800}e^{-3z}(3\cos z - 13\sin z) - \frac{1}{32}z^2e^{-z}(\sin z - \cos z) - \frac{1}{160}ze^{-z}(48\cos z + 21\sin z) + \frac{1}{3200}e^{-z}(1634\sin z - 174\cos z),$$

$$\dot{B}_3 = \frac{3}{20}ze^{-2z} - \frac{27}{100}e^{-2z} + \frac{1}{400}e^{-3z}(2\cos z - 21\sin z) - \frac{1}{16}z^2e^{-z}\cos z + \frac{1}{160}ze^{-z}(37\cos z + 59\sin z) + \frac{1}{400}e^{-z}(106\cos z - 235\sin z), \tag{14}$$

$$D_3 = -\frac{1}{20}ze^{-z} + \frac{19}{100}e^{-2z} + \frac{1}{16}z^2e^{-z}\sin z + \frac{1}{160}ze^{-z}(39\cos z - 17\sin z) - \frac{1}{400}e^{-z}(65\cos z + 46\sin z) - \frac{1}{400}e^{-3z}(11\cos z - 18\sin z),$$

from which the asymptotic vertical velocity to the third order is:

$$w = \frac{1}{2}k - \frac{7}{40}k^2 + \frac{15}{320}k^3. \tag{15}$$

The series in $k$ seems to be converging fairly rapidly, at least for $k < 1$. To check this further, it would, in principle, be possible to continue the solution in closed form to higher orders. However, the labor involved is prohibitive. For this reason, it was decided to extend the solution by use of numerical methods.

Equation (9) is of the form:

$$\tfrac{1}{2}\ddot{B}_n + D_n = H_n(B_i, \dot{B}_i, \ddot{B}_i),$$

$$\tfrac{1}{2}\ddot{D}_n - \dot{B}_n = K_n(B_i, \dot{B}_i, D_i, \dot{D}_i), \tag{16}$$

$$\text{for} \quad 1 \leqslant i \leqslant n-1.$$

TABLE 1. *Successive approximations for* $w(z)$. *All quantities are non-dimensional and* $w \approx -\sum_{n=1}^{5} B_n k^n$.

| $z$ | $B_1$ | $B_2$ | $B_3$ | $B_4$ | $B_5$ |
|---|---|---|---|---|---|
| 0.00 | 0.00000 | 0.00000 | 0.00000 | 0.00000 | 0.00000 |
| 0.25 | +0.02637 | −0.00153 | −0.00004 | +0.00008 | −0.00002 |
| 0.50 | +0.08847 | −0.00584 | −0.00017 | +0.00032 | −0.00007 |
| 0.75 | +0.16620 | −0.01255 | −0.00036 | +0.00068 | −0.00015 |
| 1.00 | +0.24584 | −0.02143 | −0.00049 | +0.00114 | −0.00026 |
| 1.25 | +0.31889 | −0.03232 | −0.00039 | +0.00164 | −0.00040 |
| 1.50 | +0.38082 | −0.04508 | +0.00011 | +0.00216 | −0.00058 |
| 1.75 | +0.42999 | −0.05937 | +0.00116 | +0.00265 | −0.00078 |
| 2.00 | +0.46663 | −0.07474 | +0.00284 | +0.00309 | −0.00103 |
| 2.25 | +0.49210 | −0.09059 | +0.00515 | +0.00346 | −0.00130 |
| 2.50 | +0.50832 | −0.10628 | +0.00805 | +0.00373 | −0.00160 |
| 2.75 | +0.51734 | −0.12121 | +0.01144 | +0.00388 | −0.00192 |
| 3.00 | +0.52113 | −0.13485 | +0.01517 | +0.00389 | −0.00223 |
| 3.25 | +0.52137 | −0.14683 | +0.01911 | +0.00374 | −0.00252 |
| 3.50 | +0.51944 | −0.15691 | +0.02311 | +0.00343 | −0.00278 |
| 3.75 | +0.51637 | −0.16504 | +0.02704 | +0.00296 | −0.00299 |
| 4.00 | +0.51292 | −0.17125 | +0.03078 | +0.00233 | −0.00314 |
| 4.25 | +0.50956 | −0.17571 | +0.03424 | +0.00157 | −0.00324 |
| 4.50 | +0.50660 | −0.17865 | +0.03736 | +0.00070 | −0.00327 |
| 4.75 | +0.50416 | −0.18034 | +0.04008 | −0.00024 | −0.00324 |
| 5.00 | +0.50227 | −0.18105 | +0.04238 | −0.00122 | −0.00316 |
| 5.25 | +0.50091 | −0.18105 | +0.04426 | −0.00220 | −0.00303 |
| 5.50 | +0.49999 | −0.18056 | +0.04574 | −0.00316 | −0.00286 |
| 5.75 | +0.49944 | −0.17980 | +0.04685 | −0.00406 | −0.00265 |
| 6.00 | +0.49916 | −0.17891 | +0.04764 | −0.00487 | −0.00242 |
| 6.25 | +0.49907 | −0.17800 | +0.04815 | −0.00560 | −0.00218 |
| 6.50 | +0.49910 | −0.17716 | +0.04842 | −0.00621 | −0.00193 |
| 6.75 | +0.49921 | −0.17643 | +0.04851 | −0.00673 | −0.00168 |
| 7.00 | +0.49936 | −0.17584 | +0.04846 | −0.00713 | −0.00144 |
| 7.25 | +0.49951 | −0.17538 | +0.04833 | −0.00744 | −0.00121 |
| 7.50 | +0.49964 | −0.17506 | +0.04814 | −0.00767 | −0.00098 |
| 7.75 | +0.49976 | −0.17484 | +0.04792 | −0.00782 | −0.00078 |
| 8.00 | +0.49986 | −0.17471 | +0.04770 | −0.00791 | −0.00060 |
| 8.25 | +0.49993 | −0.17466 | +0.04749 | −0.00795 | −0.00043 |
| 8.50 | +0.49998 | −0.17465 | +0.04730 | −0.00797 | −0.00028 |
| 8.75 | +0.50001 | −0.17467 | +0.04714 | −0.00796 | −0.00015 |
| 9.00 | +0.50003 | −0.17472 | +0.04701 | −0.00795 | −0.00004 |
| 9.25 | +0.50004 | −0.17477 | +0.04692 | −0.00793 | +0.00003 |
| 9.50 | +0.50004 | −0.17483 | +0.04685 | −0.00792 | +0.00008 |
| 9.75 | +0.50004 | −0.17488 | +0.04680 | −0.00791 | +0.00010 |
| 10.00 | +0.50003 | −0.17492 | +0.04678 | −0.00791 | +0.00012 |
| ∞ (Est.) | +0.5000 | −0.1750 | +0.0469 | −0.0080 | +0.0002 |

To obtain the fourth-order solution ($n = 4$) the functions $H_n(z)$ and $K_n(z)$ were evaluated from the analytical forms of the first, second, and third order solutions (equations 11, 12, and 14). To obtain higher order solutions ($n > 4$) the results of previous numerical computations were also used. We let $z = 10.00$ be the upper limit of computation, and chose the increment in $z$ to be 0.025. Thus, there were 400 steps between ground level and the "top" of the frictional layer, which in the theory is unbounded.

An iterative method was used to solve the linear differential equation (16). Two boundary conditions were given at infinity, and three ($B_n = \dot{B}_n = D_n = 0$) are specified at ground level. In order to carry out numerical integration step by step upward from the ground, it was necessary to assume reasonable values of $\ddot{B}_n$ and $\dot{D}_n$ at the ground as two additional boundary conditions. In general, exponentially increasing solutions were excited due to the incorrect $\ddot{B}_n(0)$ and $\dot{D}_n(0)$. However, since the differential equations are linear, corrections could be

TABLE 2. *Successive approximations for $u(x,z)$. All quantities are non-dimensional and* $u \approx \sum_{n=1}^{5} \dot{B}_n k^n x$.

| $z$ | $\dot{B}_1$ | $\dot{B}_2$ | $\dot{B}_3$ | $\dot{B}_4$ | $\dot{B}_5$ |
|---|---|---|---|---|---|
| 0.00 | 0.00000 | 0.00000 | 0.00000 | 0.00000 | 0.00000 |
| 0.25 | −0.19268 | +0.01199 | +0.00034 | −0.00065 | +0.00015 |
| 0.50 | −0.29079 | +0.02227 | +0.00069 | −0.00122 | +0.00027 |
| 0.75 | −0.32198 | +0.03126 | +0.00074 | −0.00166 | +0.00039 |
| 1.00 | −0.30956 | +0.03963 | +0.00019 | −0.00195 | +0.00050 |
| 1.25 | −0.27189 | +0.04746 | −0.00109 | −0.00207 | +0.00062 |
| 1.50 | −0.22257 | +0.05436 | −0.00303 | −0.00204 | +0.00076 |
| 1.75 | −0.17099 | +0.05969 | −0.00543 | −0.00189 | +0.00091 |
| 2.00 | −0.12306 | +0.06286 | −0.00801 | −0.00164 | +0.00105 |
| 2.25 | −0.08201 | +0.06351 | −0.01048 | −0.00129 | +0.00116 |
| 2.50 | −0.04913 | +0.06162 | −0.01264 | −0.00085 | +0.00124 |
| 2.75 | −0.02440 | +0.05744 | −0.01432 | −0.00033 | +0.00126 |
| 3.00 | −0.00703 | +0.05144 | −0.01544 | +0.00027 | +0.00121 |
| 3.25 | +0.00420 | +0.04422 | −0.01597 | +0.00091 | +0.00110 |
| 3.50 | +0.01059 | +0.03641 | −0.01595 | +0.00157 | +0.00094 |
| 3.75 | +0.01344 | +0.02858 | −0.01541 | +0.00221 | +0.00074 |
| 4.00 | +0.01386 | +0.02121 | −0.01447 | +0.00279 | +0.00050 |
| 4.25 | +0.01277 | +0.01464 | −0.01319 | +0.00328 | +0.00025 |
| 4.50 | +0.01086 | +0.00908 | −0.01168 | +0.00364 | +0.00001 |
| 4.75 | +0.00865 | +0.00462 | −0.01005 | +0.00387 | −0.00022 |
| 5.00 | +0.00646 | +0.00125 | −0.00837 | +0.00395 | −0.00043 |
| 5.25 | +0.00451 | −0.00111 | −0.00672 | +0.00389 | −0.00061 |
| 5.50 | +0.00288 | −0.00261 | −0.00517 | +0.00372 | −0.00076 |
| 5.75 | +0.00162 | −0.00340 | −0.00377 | +0.00344 | −0.00087 |
| 6.00 | +0.00069 | −0.00366 | −0.00254 | +0.00309 | −0.00095 |
| 6.25 | +0.00006 | −0.00353 | −0.00152 | +0.00269 | −0.00099 |
| 6.50 | −0.00032 | −0.00316 | −0.00070 | +0.00226 | −0.00100 |
| 6.75 | −0.00053 | −0.00265 | −0.00007 | +0.00184 | −0.00099 |
| 7.00 | −0.00060 | −0.00210 | +0.00038 | +0.00143 | −0.00096 |
| 7.25 | −0.00058 | −0.00156 | +0.00068 | +0.00106 | −0.00091 |
| 7.50 | −0.00052 | −0.00108 | +0.00084 | +0.00074 | −0.00084 |
| 7.75 | −0.00043 | −0.00067 | +0.00090 | +0.00047 | −0.00078 |
| 8.00 | −0.00033 | −0.00035 | +0.00088 | +0.00026 | −0.00071 |
| 8.25 | −0.00024 | −0.00011 | +0.00080 | +0.00011 | −0.00063 |
| 8.50 | −0.00016 | −0.00005 | +0.00069 | +0.00000 | −0.00055 |
| 8.75 | −0.00010 | +0.00015 | +0.00057 | −0.00005 | −0.00047 |
| 9.00 | −0.00005 | +0.00020 | +0.00044 | −0.00007 | −0.00038 |
| 9.25 | −0.00002 | +0.00022 | +0.00033 | −0.00006 | −0.00027 |
| 9.50 | +0.00000 | +0.00021 | +0.00022 | −0.00004 | −0.00014 |
| 9.75 | +0.00002 | +0.00019 | +0.00013 | −0.00001 | +0.00002 |
| 10.00 | +0.00002 | +0.00015 | +0.00006 | −0.00001 | +0.00016 |
| ∞ (Est.) | 0.00000 | 0.00000 | 0.00000 | 0.00000 | 0.00000 |

mathematically computed and new estimates of $B_n$ and $D_n$ at the ground could be obtained. The procedure was then repeated with the improved estimates. By using this procedure and a 5-point formula for upward integration, it was found that the exponentially increasing terms could be eliminated after a few iterations, and the higher order solution for $B_n$ and $D_n$ could be obtained.

Although this numerical method could in principle be repeated indefinitely, the series converged rapidly and errors accumulated slowly. It was apparent that little would be gained by extending the computation beyond the fifth order unless a deeper layer were used.

The numerical values of $B_n$, $\dot{B}_n$ and $D_n$ for $1 \leqslant n \leqslant 5$ are given in Tables 1, 2 and 3, at intervals of 0.25 in $z$. It is to be noted that the coefficients of the powers of $k$ decrease rapidly. There appears to be a radius of convergence

TABLE 3. *Successive approximations for $v(x,z)$. All quantities are non-dimensional, and* $v \approx \sum_{n=1}^{5} D_n k^n x$.

| $z$ | $D_1$ | $D_2$ | $D_3$ | $D_4$ | $D_5$ |
|---|---|---|---|---|---|
| 0.00 | 0.00000 | 0.00000 | 0.00000 | 0.00000 | 0.00000 |
| 0.25 | +0.24541 | +0.03749 | −0.00283 | −0.00040 | +0.00027 |
| 0.50 | +0.46772 | +0.07349 | −0.00584 | −0.00081 | +0.00056 |
| 0.75 | +0.65437 | +0.10441 | −0.00921 | −0.00117 | +0.00085 |
| 1.00 | +0.80123 | +0.12691 | −0.01290 | −0.00140 | +0.00112 |
| 1.25 | +0.90966 | +0.13913 | −0.01671 | −0.00141 | +0.00134 |
| 1.50 | +0.98422 | +0.14092 | −0.02036 | −0.00115 | +0.00149 |
| 1.75 | +1.03097 | +0.13354 | −0.02355 | −0.00058 | +0.00155 |
| 2.00 | +1.05632 | +0.11914 | −0.02606 | +0.00029 | +0.00150 |
| 2.25 | +1.06621 | +0.10024 | −0.02772 | +0.00140 | +0.00135 |
| 2.50 | +1.06576 | +0.07929 | −0.02843 | +0.00266 | +0.00112 |
| 2.75 | +1.05909 | +0.05840 | −0.02818 | +0.00397 | +0.00082 |
| 3.00 | +1.04929 | +0.03917 | −0.02705 | +0.00522 | +0.00047 |
| 3.25 | +1.03855 | +0.02265 | −0.02507 | +0.00630 | +0.00010 |
| 3.50 | +1.02828 | +0.00938 | −0.02247 | +0.00713 | −0.00027 |
| 3.75 | +1.01930 | −0.00053 | −0.01941 | +0.00766 | −0.00064 |
| 4.00 | +1.01197 | −0.00728 | −0.01611 | +0.00788 | −0.00097 |
| 4.25 | +1.00636 | −0.01129 | −0.01274 | +0.00779 | −0.00127 |
| 4.50 | +1.00234 | −0.01309 | −0.00950 | +0.00742 | −0.00153 |
| 4.75 | +0.99967 | −0.01322 | −0.00651 | +0.00683 | −0.00173 |
| 5.00 | +0.99809 | −0.01221 | −0.00390 | +0.00607 | −0.00187 |
| 5.25 | +0.99731 | −0.01053 | −0.00173 | +0.00520 | −0.00194 |
| 5.50 | +0.99710 | −0.00852 | −0.00002 | +0.00429 | −0.00196 |
| 5.75 | +0.99726 | −0.00648 | +0.00123 | +0.00339 | −0.00191 |
| 6.00 | +0.99761 | −0.00458 | +0.00206 | +0.00253 | −0.00181 |
| 6.25 | +0.99807 | −0.00294 | +0.00252 | +0.00175 | −0.00166 |
| 6.50 | +0.99853 | −0.00162 | +0.00268 | +0.00107 | −0.00148 |
| 6.75 | +0.99895 | −0.00061 | +0.00261 | +0.00051 | −0.00127 |
| 7.00 | +0.99931 | +0.00009 | +0.00238 | +0.00006 | −0.00106 |
| 7.25 | +0.99960 | +0.00054 | +0.00205 | −0.00028 | −0.00084 |
| 7.50 | +0.99981 | +0.00079 | +0.00167 | −0.00052 | −0.00063 |
| 7.75 | +0.99996 | +0.00088 | +0.00128 | −0.00066 | −0.00045 |
| 8.00 | +1.00005 | +0.00086 | +0.00092 | −0.00073 | −0.00030 |
| 8.25 | +1.00010 | +0.00077 | +0.00060 | −0.00074 | −0.00018 |
| 8.50 | +1.00012 | +0.00064 | +0.00033 | −0.00069 | −0.00010 |
| 8.75 | +1.00012 | +0.00050 | +0.00013 | −0.00060 | −0.00006 |
| 9.00 | +1.00011 | +0.00037 | −0.00003 | −0.00048 | −0.00004 |
| 9.25 | +1.00009 | +0.00025 | −0.00013 | −0.00034 | −0.00003 |
| 9.50 | +1.00007 | +0.00015 | −0.00019 | −0.00017 | −0.00002 |
| 9.75 | +1.00006 | +0.00008 | −0.00021 | +0.00002 | +0.00001 |
| 10.00 | +1.00004 | +0.00002 | −0.00021 | +0.00022 | +0.00009 |
| ∞ (Est.) | +1.00000 | 0.00000 | 0.00000 | 0.00000 | 0.00000 |

which may even extend to $k = -1$ and $k > 1$. However, the general form of the coefficients of the series cannot be obtained, and it is therefore not possible to establish the radius of convergence with rigor.

Tables 4 and 5 present the non-dimensional velocity components $u$, $v$, $w$ for $k = +1.0$ and $k = -1.0$. The results are also plotted in Figs. 1 and 2, respectively. The substantial differences between the cases of cyclonic shear ($k > 0$) and anticyclonic shear ($k < 0$) are evident. Vertical motions are stronger with anticyclonic relative vorticity, when flows with equal magnitudes of shear are compared.

This is especially apparent from the approximate expression for the asymptotic vertical velocity:

$$w \approx \frac{1}{2}k - \frac{7}{40}k^2 + \frac{15}{320}k^3 - \frac{8}{1000}k^4 + \frac{2}{10{,}000}k^5. \quad (17)$$

TABLE 4. *Fifth order approximations for $w(z)$, $u/x$, and $v/x$ for $k = +1.00$.*

| $z$ | $w$ | $u/x$ | $v/x$ |
|---|---|---|---|
| 0.00 | 0.00000 | 0.00000 | 0.00000 |
| 0.25 | +0.02486 | −0.18085 | +0.27995 |
| 0.50 | +0.08270 | −0.26878 | +0.53512 |
| 0.75 | +0.15381 | −0.29126 | +0.74926 |
| 1.00 | +0.22480 | −0.27119 | +0.91496 |
| 1.25 | +0.28741 | −0.22696 | +1.03200 |
| 1.50 | +0.33743 | −0.17252 | +1.10511 |
| 1.75 | +0.37364 | −0.11772 | +1.14193 |
| 2.00 | +0.39679 | −0.06880 | +1.15119 |
| 2.25 | +0.40882 | −0.02911 | +1.14148 |
| 2.50 | +0.41221 | +0.00024 | +1.12090 |
| 2.75 | +0.40953 | +0.01965 | +1.09410 |
| 3.00 | +0.40311 | +0.03046 | +1.06710 |
| 3.25 | +0.39487 | +0.03446 | +1.04253 |
| 3.50 | +0.38628 | +0.03358 | +1.02260 |
| 3.75 | +0.37834 | +0.02956 | +1.00638 |
| 4.00 | +0.37164 | +0.02390 | +0.99549 |
| 4.25 | +0.36643 | +0.01775 | +0.98885 |
| 4.50 | +0.36274 | +0.01190 | +0.98565 |
| 4.75 | +0.36041 | +0.00686 | +0.98504 |
| 5.00 | +0.35922 | +0.00286 | +0.98617 |
| 5.25 | +0.35889 | −0.00004 | +0.98832 |
| 5.50 | +0.35916 | −0.00194 | +0.99089 |
| 5.75 | +0.35979 | −0.00299 | +0.99349 |
| 6.00 | +0.36060 | −0.00337 | +0.99582 |
| 6.25 | +0.36144 | −0.00329 | +0.99774 |
| 6.50 | +0.36225 | −0.00292 | +0.99919 |
| 6.75 | +0.36286 | −0.00239 | +1.00019 |
| 7.00 | +0.36341 | −0.00184 | +1.00079 |
| 7.25 | +0.36380 | −0.00131 | +1.00107 |
| 7.50 | +0.36407 | −0.00086 | +1.00112 |
| 7.75 | +0.36424 | −0.00051 | +1.00100 |
| 8.00 | +0.36433 | −0.00025 | +1.00079 |
| 8.25 | +0.36437 | −0.00009 | +1.00055 |
| 8.50 | +0.36438 | −0.00000 | +1.00023 |
| 8.75 | +0.36436 | +0.00010 | +1.00009 |
| 9.00 | +0.36433 | +0.00015 | +0.99994 |
| 9.25 | +0.36428 | +0.00020 | +0.99985 |
| 9.50 | +0.36423 | +0.00026 | +0.99985 |
| 9.75 | +0.36415 | +0.00037 | +0.99995 |
| 10.00 | +0.36406 | +0.00035 | +1.00016 |
| ∞ (Est.) | +0.3640 | 0.0000 | +1.0000 |

TABLE 5. *Fifth order approximations for $w(z)$, $u/x$, and $v/x$ for $k = -1.00$.*

| $z$ | $w$ | $u/x$ | $v/x$ |
|---|---|---|---|
| 0.00 | 0.00000 | 0.00000 | 0.00000 |
| 0.25 | −0.02775 | +0.20353 | −0.20577 |
| 0.50 | −0.09375 | +0.31088 | −0.39006 |
| 0.75 | −0.17756 | +0.35046 | −0.54278 |
| 1.00 | −0.26537 | +0.34655 | −0.66395 |
| 1.25 | −0.34877 | +0.31775 | −0.75657 |
| 1.50 | −0.42327 | +0.27716 | −0.82558 |
| 1.75 | −0.48709 | +0.23332 | −0.87600 |
| 2.00 | −0.54009 | +0.19124 | −0.91233 |
| 2.25 | −0.58308 | +0.15356 | −0.93821 |
| 2.50 | −0.61732 | +0.12131 | −0.95649 |
| 2.75 | −0.64419 | +0.09458 | −0.96835 |
| 3.00 | −0.66504 | +0.07297 | −0.97832 |
| 3.25 | −0.68105 | +0.05581 | −0.98463 |
| 3.50 | −0.69326 | +0.04240 | −0.98902 |
| 3.75 | −0.70250 | +0.03204 | −0.99211 |
| 4.00 | −0.70948 | +0.02410 | −0.99429 |
| 4.25 | −0.71472 | +0.01808 | −0.99586 |
| 4.50 | −0.71864 | +0.01353 | −0.99698 |
| 4.75 | −0.72157 | +0.01011 | −0.99783 |
| 5.00 | −0.72376 | +0.00753 | −0.99847 |
| 5.25 | −0.72539 | +0.00560 | −0.99896 |
| 5.50 | −0.72660 | +0.00415 | −0.99935 |
| 5.75 | −0.72750 | +0.00306 | −0.99966 |
| 6.00 | −0.72816 | +0.00223 | −0.99991 |
| 6.25 | −0.72863 | +0.00160 | −1.00012 |
| 6.50 | −0.72897 | +0.00113 | −1.00028 |
| 6.75 | −0.72920 | +0.00077 | −1.00040 |
| 7.00 | −0.72936 | +0.00050 | −1.00049 |
| 7.25 | −0.72946 | +0.00032 | −1.00054 |
| 7.50 | −0.72952 | +0.00019 | −1.00057 |
| 7.75 | −0.72956 | +0.00011 | −1.00057 |
| 8.00 | −0.72958 | +0.00007 | −1.00054 |
| 8.25 | −0.72960 | +0.00006 | −1.00049 |
| 8.50 | −0.72962 | +0.00003 | −1.00040 |
| 8.75 | −0.72964 | +0.00009 | −1.00029 |
| 9.00 | −0.72966 | +0.00011 | −1.00016 |
| 9.25 | −0.72968 | +0.00012 | −1.00002 |
| 9.50 | −0.72970 | +0.00008 | −0.99988 |
| 9.75 | −0.72971 | +0.00003 | −0.99976 |
| 10.00 | −0.72972 | +0.00000 | −0.99968 |
| ∞ (Est.) | −0.7297 | 0.0000 | −1.0000 |

This fifth order solution is compared with the first and second order results in Fig. 3. It may be noted that for $k = -1.0$ the magnitude of the asymptotic vertical velocity is almost exactly double the value for $k = +1.0$.

Geophysical interpretations of the above results will be presented in a later section.

## 4. General case with horizontal shear in both $x$ and $y$

In this section we consider the more general case for which the horizontal velocity has a linear shear in both $x$ and $y$. The velocity components and the pressure have the form given by (2) with $E = F = 0$ from symmetry considerations. Again steady state will be assumed and the variables are non-dimensionalized as given by (4).

As previously stated, the boundary conditions are that the fluid velocity vanishes at $z = 0$, and the flow becomes non-divergent, and independent of $z$, as $z \to \infty$. Thus divergence is only caused by friction in the boundary layer. The net effect of the divergence (or convergence) is to give a constant vertical velocity as $z \to \infty$.

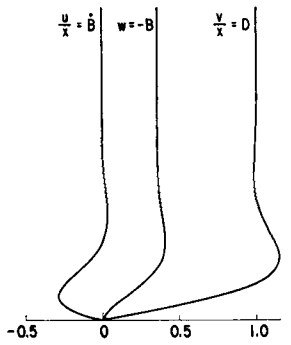


FIG. 1. The functions $u(z)/x$; $w(z)$; and $v(z)/x$ for $k = +1.0$.

As in the previous section, the dependent variables can be expanded in an infinite series and an approximate solution obtained. This approach will be discussed later. First we obtain the exact solution for the horizontal velocities as $z \to \infty$. From the boundary conditions, equations (5) reduce to

$$\begin{aligned} \dot{B}^2 + AD &= -k + D, \\ 0 &= \dot{C}, \\ 0 &= -\dot{B}, \\ \dot{C}^2 + AD &= m - A. \end{aligned} \tag{18}$$

As $z \to \infty$, $B$ and $C$ approach zero. Thus we have:

$$\begin{aligned} u &= Ay, \\ v &= Dx, \end{aligned} \tag{19}$$

where $A$ and $D$ are constants determined by the equations

$$\begin{aligned} AD &= -k + D, \\ AD &= m - A. \end{aligned} \tag{20}$$

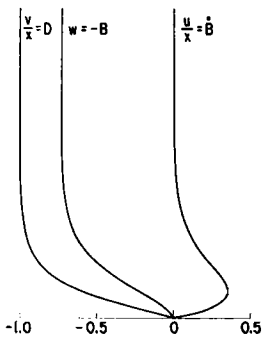


FIG. 2. The functions $u(z)/x$; $w(z)$; and $v(z)/x$ for $k = -1.0$.

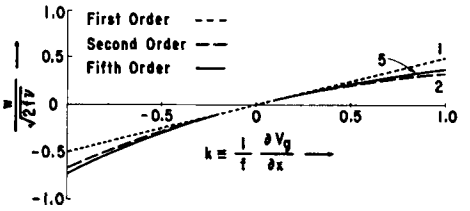


FIG. 3. The non-dimensional vertical wind speed at the top of the friction layer, as a function of the horizontal shear in the geostrophic wind velocity, $f^{-1}\partial(v_g)/\partial x$.

The above are two non-linear equations from which the values of $A$ and $D$ can be found for given values of $k$ and $m$. Since the equations are non-linear, we find two possible pairs of values of $D$ and $A$:

$$\begin{aligned} D &= \frac{k + m - 1 \pm \sqrt{(k+m)^2 + 2(k-m) + 1}}{2}, \\ A &= \frac{k + m + 1 \mp \sqrt{(k+m)^2 + 2(k-m) + 1}}{2}. \end{aligned} \tag{21}$$

In order to gain physical insight into the nature of the two types of solutions, we consider the angular deformation $D + A$ and the relative vorticity $D - A$. For either type of solution the angular deformation is:

$$D + A = k + m \tag{22}$$

which result could be obtained from (20) directly. The relative vorticity has the two possible values:

$$\begin{aligned} D - A &= -1 + \sqrt{(k+m)^2 + 2(k-m) + 1}. \quad \text{(a)} \\ D - A &= -1 - \sqrt{(k+m)^2 + 2(k-m) + 1}. \quad \text{(b)} \end{aligned} \tag{23}$$

This result shows the basic difference between the two types of asymptotic flows. If we consider (23*a*)—which corresponds to the positive root in $D$ and the negative root in $A$—the non-dimensional relative vorticity is always greater than $-1$ as long as the quantity inside the radical is positive. In equation (23*b*)—which corresponds to the negative root in $D$ and the positive root in $A$—the relative vorticity is less than $-1$ for the same values of $k$ and $m$. For this case the absolute vorticity is negative.

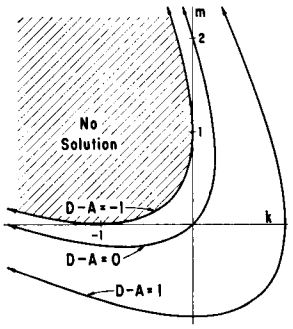


FIG. 4. The distribution of asymptotic relative vorticity $(D-A)$ in the $(k, m)$ plane.

It seems evident that solutions with negative absolute vorticity will not be of physical interest. ROGERS and LANCE (1960) find that a steady solution ceases to exist for the case of circular symmetry when $D-A \leqslant -1.2$ unless suction is applied at the ground. It may also be noted, in the case of circular symmetry, that anticyclonic vorticity is associated with low pressure when $D-A \leqslant -2$. In large scale geophysical motions such a state is never observed. In fact, negative absolute vorticity is seldom found. An exception may occur in the atmosphere just south of the jet stream, but this is in the upper atmosphere and not just above the friction layer, which is the region discussed here. For these reasons we will not consider the solutions with negative absolute vorticity any further.

It is of interest to note that there is a certain range of values of $k$ and $m$ for which no solution exists. These are the values of $k$ and $m$ for which the quantity under the radical in (21) becomes negative. This region in the $(k, m)$-plane is bounded by the curve for which the radical term vanishes, along which the absolute vorticity is zero. The equation of the curve is:

$$(k+m)^2 + 2(k-m) + 1 = 0, \tag{24}$$

or solving for $k$ in terms of $m$:

$$k = -(1 \pm m^{\frac{1}{2}})^2. \tag{25}$$

It is seen that the curve given by (25) exists only for positive $m$ and negative $k$. This curve and the region where no solutions exist are shown in Fig. 4.

In the same figure we show the sign of the relative vorticity at $z=\infty$ throughout the $(k, m)$-plane. It is noted that the negative relative vorticity is contained in a narrow region between the $D-A=-1$ and the $D-A=0$ curves. The majority of the $(k, m)$-plane has positive values of $D-A$ and the region for which $0 < D-A < 1$ is considerably larger than the region for which the relative vorticity is negative.

It is now shown that the solutions (21) for $D$ and $A$ become geostrophic as $k, m \to 0$. Since we only consider the solutions with the plus sign in front of the radical for $D$ and the minus sign for $A$, we find in the limit as $k, m \to 0$:

$$\begin{aligned} D &\to k \\ A &\to m. \end{aligned} \tag{26}$$

This result suggests that we expand the dependent variables in infinite series in $k$ and $m$. In order that we need only expand in one parameter, we set $m = \gamma k$ and expand the four dependent variables as infinite series in $k$.

$$\begin{aligned} A &= \sum_{n=1}^{\infty} k^n A_n(z), \quad B = \sum_{n=1}^{\infty} k^n B_n(z), \\ C &= \sum_{n=1}^{\infty} k^n C_n(z), \quad D = \sum_{n=1}^{\infty} k^n D_n(z). \end{aligned} \tag{27}$$

It is seen from (5) that the lowest order terms $A$, $B$, $C$ and $D$ are given by the solution to the equations:

$$\begin{aligned} 0 &= -1 + D_1 + \tfrac{1}{2}\ddot{B}_1, \\ 0 &= \quad \dot{C}_1 + \tfrac{1}{2}\ddot{A}_1, \\ 0 &= \quad -\dot{B}_1 + \tfrac{1}{2}\ddot{D}_1, \\ 0 &= \gamma - A_1 + \tfrac{1}{2}\ddot{C}_1, \end{aligned} \tag{28}$$

where we have set $m = \gamma k$ and the dots are again used to represent differentiation with respect to $z$.

The boundary conditions are:

$$\begin{aligned} &\text{at } z=0 : A_1 = B_1 = C_1 = D_1 = \dot{B}_1 = \dot{C}_1 = 0. \\ &\text{at } z=\infty: D_1 = 1, A_1 = \gamma, \dot{B}_1 = \dot{C}_1 = 0. \end{aligned} \tag{29}$$

The above four equations separate into two sets of two equations and can be solved readily. The solutions are:

$$
\begin{aligned}
B_1 &= -\tfrac{1}{2}[1-e^{-z}(\cos z+\sin z)],\\
\dot{B}_1 &= -e^{-z}\sin z,\\
D_1 &= 1-e^{-z}\cos z,\\
C_1 &= \tfrac{1}{2}\gamma[1-e^{-z}(\cos z+\sin z)],\\
\dot{C}_1 &= \gamma e^{-z}\sin z,\\
A_1 &= \gamma(1-e^{-z}\cos z).
\end{aligned}
\tag{30}
$$

As in the previous case with $m=0$, the above solutions are similar to those of the Ekman problem, except that horizontal velocity shears are present which give rise to a vertical velocity. Since to this order the effects of the velocity shears in $x$ and $y$ are decoupled, each gives rise to its respective vertical velocity. The total non-dimensional vertical velocity is given by

$$
w=\frac{k(1-\gamma)}{2}=\frac{k-m}{2}. \tag{31}
$$

The relative vorticity at $z=\infty$ to the same order is given by:

$$
D-A=k-m. \tag{32}
$$

Hence to the first order the vertical velocity is proportional to the first order relative vorticity with upward motion for cyclonic vorticity and downward motion for anticyclonic vorticity. Unlike the previous case with $m=0$, the first order relative vorticity at $z=\infty$ is not equal to the exact relative vorticity. The exact value is given by (23*a*).

These results can be extended to obtain the second order solution. The coefficients of the parameter $k^2$ yield the following equations:

$$
\begin{aligned}
D_2+\tfrac{1}{2}\ddot{B}_2 &= \dot{B}_1^2-B_1\ddot{B}_1+A_1D_1-\ddot{B}_1C_1,\\
-\dot{B}_2+\tfrac{1}{2}\dddot{D}_2 &= \ddot{B}_1D_1-B_1\dot{D}_1+\dot{C}_1D_1-C_1\dot{D}_1,\\
-A_2+\tfrac{1}{2}\ddot{C}_2 &= \dot{C}_1^2-C_1\ddot{C}_1+A_1D_1-B_1\ddot{C}_1,\\
\dot{C}_2+\tfrac{1}{2}\dddot{A}_2 &= A_1\ddot{B}_1-\dot{A}_1B_1+A_1\dot{C}_1-\dot{A}_1C_1.
\end{aligned}
\tag{33}
$$

After a straightforward but lengthy integration one obtains:

$$
\begin{aligned}
B_2 &= \frac{7-21\gamma}{40}-\frac{\gamma+3}{20}e^{-2z}-\frac{\gamma-1}{4}ze^{-z}\cos z\\
&\quad+\frac{\gamma}{2}ze^{-z}\sin z+\frac{23\gamma-1}{40}e^{-z}\cos z\\
&\quad+\frac{29\gamma-23}{40}e^{-z}\sin z,
\end{aligned}
$$

$$
\begin{aligned}
D_2 &= \gamma+\frac{3\gamma-1}{10}e^{-2z}-\frac{\gamma+1}{4}ze^{-z}\cos z\\
&\quad-\frac{3\gamma-1}{4}ze^{-z}\sin z+\frac{1-13\gamma}{10}e^{-z}\cos z\\
&\quad+\frac{\gamma+3}{10}e^{-z}\sin z,
\end{aligned}
$$

$$
\begin{aligned}
\dot{B}_2 &= \frac{\gamma+3}{10}e^{-2z}+\frac{3\gamma-1}{4}ze^{-z}\cos z-\frac{\gamma+1}{4}ze^{-z}\sin z\\
&\quad-\frac{\gamma+3}{10}e^{-z}\cos z-\frac{8\gamma-6}{10}e^{-z}\sin z,
\end{aligned}
\tag{34}
$$

$$
\begin{aligned}
C_2 &= \frac{7\gamma^2-21\gamma}{40}-\frac{\gamma+3\gamma^2}{20}e^{-2z}+\frac{\gamma^2-\gamma}{4}ze^{-z}\cos z\\
&\quad+\frac{\gamma}{2}ze^{-z}\sin z-\frac{\gamma^2-23\gamma}{40}e^{-z}\cos z\\
&\quad-\frac{23\gamma^2-29\gamma}{40}e^{-z}\sin z,
\end{aligned}
$$

$$
\begin{aligned}
A_2 &= -\gamma+\frac{\gamma^2-3\gamma}{10}e^{-2z}+\frac{\gamma^2+\gamma}{4}ze^{-z}\cos z\\
&\quad-\frac{\gamma^2-3\gamma}{4}ze^{-z}\sin z-\frac{\gamma^2-13\gamma}{10}e^{-z}\cos z\\
&\quad-\frac{3\gamma^2+\gamma}{10}e^{-z}\sin z,
\end{aligned}
$$

$$
\begin{aligned}
\dot{C}_2 &= \frac{3\gamma^2+\gamma}{10}e^{-2z}-\frac{\gamma^2-3\gamma}{4}ze^{-z}\cos z\\
&\quad-\frac{\gamma^2+\gamma}{4}ze^{-z}\sin z-\frac{3\gamma^2+\gamma}{10}e^{-z}\cos z\\
&\quad+\frac{6\gamma^2-8\gamma}{10}e^{-z}\sin z.
\end{aligned}
$$

From these solutions we can find to second order the relative vorticity and vertical velocity as $z\to\infty$.

$$
\begin{aligned}
&D-A=k-m+2km. && \text{(a)}\\
&w=\frac{k-m}{2}-\frac{7(k^2+m^2)-42km}{40}. && \text{(b)}
\end{aligned}
\tag{35}
$$

We now have two sets of data: (*a*) a second order solution for all $z$; and (*b*) exact values of

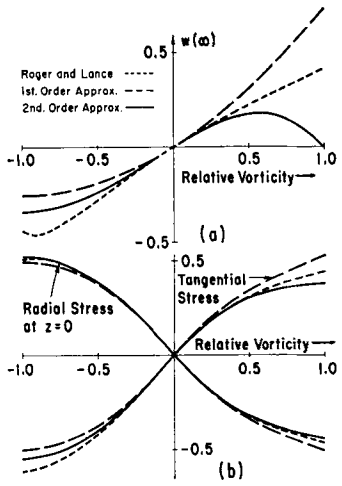


FIG. 5. (*a*) Non-dimensional vertical velocity $[w(2fv)^{-\frac{1}{2}}]$ as $z \to \infty$. (*b*) Non-dimensional stress components [stress/$v$ fr] at $z = 0$.

the vorticity as $z \to \infty$. The accuracy of the second order solution can be estimated in two ways: first, by comparing the solution with certain special cases for which more extensive computations are available; and second, by comparing the second-order asymptotic vorticity with the exact value.

Let us consider the former procedure. For $m = 0$ (or $k = 0$) the velocity field has been computed to the fifth order in the previous section. For this simple case of uni-directional flow at infinity, the asymptotic values of angular deformation and vorticity are exact, even for the first order solution. There are, however, differences between the second order and fifth order estimates of the asymptotic vertical velocity, and these differences vary as a function of $k$ (or $m$). This is shown in Fig. 3. The accuracy of the asymptotic estimates of vertical velocities obtained using second-order theory is excellent. The error is less than 15 % for $-1 \leqslant k \leqslant +1$.

Let us now make a similar comparison for a circular vortex, for which $m = -k$. This case was studied in detail by ROGERS and LANCE (1960). Fig. 5 shows asymptotic vertical velocity, and non-dimensional stress components (stress/$fvr$) at the ground as a function of $k$ for three sets of data: first order theory, second order theory, and the numerical solution of Rogers and Lance. The data are plotted for $-\frac{1}{4} \leqslant k \leqslant +\frac{3}{4}$, which corresponds to relative vortices ranging from $-1$ to $+1$.

It is interesting to note that the second order approximations are very good for the stress components at the ground for the range of $k$ considered. However, the second order vertical velocities seem to contain large errors for $k > 0.3$. It is relevant to mention that for $k > 0$ the range of validity of the similarity solution is in question (STEWARTSON, 1957).

We now examine the accuracy of the second order solution by comparing the second order asymptotic relative vorticity (35*a*) with the exact value (23*a*). The results are presented in Table 6 for $-0.50 \leqslant (k, m) \leqslant +0.75$. The circular

TABLE 6. *The asymptotic relative vorticity (nondimensional): exact value (top figure) compared with second order approximation (bottom figure).*

| $m/k$ | $-0.50$ | $-0.25$ | 0 | $+0.25$ | $+0.50$ | $+0.75$ |
|---|---|---|---|---|---|---|
| $-0.50$ | $+0.414$ | $+0.436$ | $+0.50$ | $+0.60$ | $+0.732$ | $+0.888$ |
| | $+0.50$ | $+0.50$ | $+0.50$ | $+0.50$ | $+0.50$ | $+0.50$ |
| $-0.25$ | $+0.03$ | $+0.119$ | $+0.25$ | $+0.414$ | $+0.60$ | $+0.803$ |
| | 0 | $+0.125$ | $+0.25$ | $+0.375$ | $+0.50$ | $+0.625$ |
| 0 | $-0.50$ | $-0.25$ | 0 | $+0.25$ | $+0.50$ | $+0.75$ |
| | $-0.50$ | $-0.25$ | 0 | $+0.25$ | $+0.50$ | $+0.75$ |
| $+0.25$ | | $-1.00$ | $-0.25$ | $+0.119$ | $+0.436$ | $+0.732$ |
| | | $-0.625$ | $-0.25$ | $+0.125$ | $+0.50$ | $+0.875$ |
| $+0.50$ | | | $-0.50$ | $+0.03$ | $+0.414$ | $+0.75$ |
| | | | $-0.50$ | 0 | $+0.50$ | $+1.00$ |
| $+0.75$ | | | $-0.75$ | 0 | $+0.436$ | $+0.803$ |
| | | | $-0.75$ | $-0.125$ | $+0.50$ | $+1.125$ |

TABLE 7. *Asymptotic relative vorticity (sec$^{-1}$) and vertical velocity (cm/sec) for different types of flow patterns. The vertical velocities are obtained from:* (1) *The fifth order approximation (Equation 17).* (2) *The second order approximation (Equation 35b).* (3) *The data of Rogers and Lance.*

| Flow Pattern | $k$ | $m$ | Vorticity | Asymptotic (1) | Vertical (2) | Velocity (3) |
|---|---|---|---|---|---|---|
| Linear Shear | +1.000 | 0 | +1.00 | +1.63 | +1.45 | — |
| | −1.000 | 0 | −1.00 | −3.27 | −3.02 | — |
| Circular Vortex | +0.312 | −0.312 | +0.50 | — | +0.79 | +1.02 |
| | −0.188 | +0.188 | −0.50 | — | −1.06 | −1.22 |
| Oblate Vortex | +0.440 | −0.140 | +0.50 | — | +0.84 | — |
| | −0.060 | +0.360 | −0.50 | — | −1.15 | — |
| Col | +0.234 | +0.516 | 0 | — | −0.32 | — |
| | +0.375 | +0.375 | +0.25 | — | +0.44 | — |
| | +0.125 | +0.625 | −0.25 | — | −1.107 | — |

vortex ($k = -m$) has the greatest errors in the second order theory, whereas values along the axes ($k = 0$ or $m = 0$) are exact. Both of these special cases have been examined previously.

It would appear that in the case of circular or nearly circular cyclonic vortices the second order solution should be used with caution for $k$ or $m$ greater in magnitude than about 0.25. This remark also applies to circular anticyclonic vortices, for which the solution ceases to exist for $k < -0.25$. For asymptotic flows which are less circular—more unidirectional in character—the accuracy of the second order theory seems to improve.

## 5. Geophysical applications

The above results will provide theoretical background for the consideration of problems of geophysical interest in both meteorology and oceanography. In the latter field, however, the Ekman layer of primary importance occurs at the ocean surface. Although the governing differential equations will be similar if density stratification is neglected, the boundary conditions will differ from those discussed above. For this reason, examples of physical application are limited to the turbulent atmospheric boundary layer.

In order to consider the meteorological significance of the above results, we calculate the vertical velocities as $z \to \infty$ for some cases of physical interest. The vertical velocities which may be set up from the boundary layer as a result of lateral shear in the horizontal velocities are not negligible. To obtain estimates of the vertical velocities, one must assume an eddy viscosity—say, $\nu = 10^5$ cm$^2$/sec. In these calculations we consider middle latitudes where $f \approx 10^{-4}$ sec$^{-1}$.

The vertical velocities are calculated for the following types of flow patterns: (*a*) linear shears in one dimension only; (*b*) circular vortices; (*c*) oblate vortices; and (*d*) cols. The results are discussed below and summarized in Table 7. To find these velocities we use the approximate solutions obtained above and the numerical data of Rogers and Lance. Where the approximate solutions are used, the resulting vertical velocities will, of course, be limited in accuracy as discussed in the previous section. However such errors are not of critical importance here: certainly a much larger source of error results from the assumption of a constant eddy viscosity parameter—a very crude approximation, indeed. All that one can hope to obtain in the results below is the approximate magnitude of the vertical velocities and a qualitatively correct comparison of the vertical velocity between the various cases considered.

The case of linear shear in one dimension only ($m = 0$) is discussed first. If we have a horizontal velocity shear of one meter per second in ten kilometers ($k = \pm 1$), we find from (17) a vertical velocity of 1.63 cm/sec with cyclonic shear and −3.27 cm/sec with anticyclonic shear. Such a velocity shear is entirely likely on a local scale, although it is larger than one normally would expect to find over wide areas near the surface of the earth.

The values of the vertical velocities for circu-

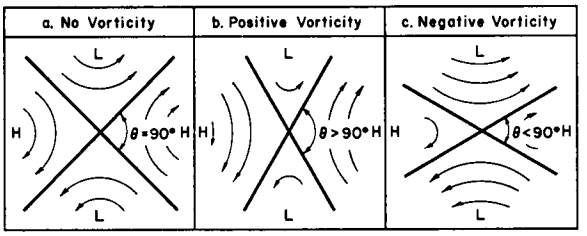


FIG. 6. A schematic representation of the three possible flow patterns in the vicinity of a col. The letters $H$ and $L$ stand for high and low pressure. The angle $\theta$ is the angle between the crossing streamline as indicated.

lar vortices and oblate vortices are shown in Table 7. For the circular vortices we calculate values from the second order theory (Equation 35*b*) and the data of Rogers and Lance. For the oblate vortices we take an oblateness of two to one, i.e., the isobars in horizontal planes as $z \to \infty$ form ellipses in which the ratio of the major to the minor axis is 2:1. The values of vertical velocity for the oblate vortices were calculated from the second order theory. All these values of vertical velocity are near one centimeter per second, and in each case the downward velocity associated with anticyclonic relative vorticity is stronger than the upward velocity associated with cyclonic relative vorticity of the same magnitude.

The final type of flow pattern considered is known as a col. This term is used to describe the flow in the immediate vicinity of a stagnation point which occurs between two high and two low pressure centers. The relative vorticity associated with a col can be either positive, negative, or zero. The flow patterns for these three cases are shown in Fig. 6. The angle $\theta$ between the crossing streamlines is given by:

$$\theta = 2 \arctan\left(\sqrt{\frac{D}{A}}\right).$$

Thus for zero relative vorticity ($D - A = 0$) we have $\theta = 90°$. Likewise for positive relative vorticity $\theta > 90°$ and for negative relative vorticity $\theta < 90°$. The vertical velocities calculated for these three cases are shown in Table 7. In each case we have taken the angular deformation ($D + A$) to be $0.75 \times 10^{-4}$ sec$^{-1}$. It is again noted that the downward velocity associated with anticyclonic relative vorticity is stronger than the upward motion associated with cyclonic vorticity of the same magnitude.

It is evident from Table 7 that for each type of flow pattern considered this same result holds. In the Introduction it was noted that if the inertia terms in the equations of motion are neglected, the resulting first order theory indicates that the vertical velocity at the top of the friction layer is proportional to the relative vorticity at the top of the friction layer (see CHARNEY and ELIASSEN, 1949). This result holds for all types of flow patterns. In the flow patterns considered above, for which linear shears exist in the horizontal velocities, it is seen that the effect of the nonlinear inertia terms is such that the downward velocities associated with negative relative vorticity are stronger than the upward velocities associated with positive relative vorticity. One may surmise—although no rigorous proof is present—that the same result may hold for other flow patterns as well.

## REFERENCES

BOEDEWADT, V. T., 1940, Die Drekstromung uber festem Grunde. *ZAMM*, Vol. 20.

CHARNEY, J. G., and ELIASSEN, A., 1949, A numerical method for predicting the perturbations of the middle latitude westerlies. *Tellus*, **1**, 2, pp. 38–54.

EKMAN, V. W., 1905, On the influence of the earth's rotation on ocean currents. *Arkiv. Mat. Astron. Fysik*, **1**, 1–2.

FALLER, A. J., 1963, An experimental study of the instability of the laminar Ekman boundary layer. *J. Fluid Mech.*, **15**, 4, pp. 560–576.

LIN, C. C., 1958, Note on a class of exact solutions in magnetohydrodynamics. *Arch. for Rational Mech. and Analysis*, **1**, 5.

ROGERS, M. H., and LANCE, G. N., 1960, The rotationally symmetric flow of a viscous fluid in the presence of an infinite rotating disk. *J. Fluid Mech.*, **7**, pp. 617–631.

STEWARTSON, K., 1957, On rotating laminar boundary layers. *Boundary Layer Research*, University of Freiburg, pp. 69–71.